Journal of Hydrology: Regional Studies 53 (2024) 101761

Contents lists available at ScienceDirect

Journal of Hydrology: Regional Studies

journal homepage: www.elsevier.com/locate/ejrh

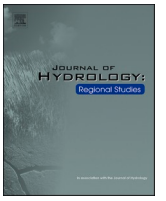

Sensitivity of Standardized Precipitation and Evapotranspiration Index (SPEI) to the choice of SPEI probability distribution and evapotranspiration method

Sanghyun Lee [a,b,*], Daniel N. Moriasi [b], Ali Danandeh Mehr [c,d], Ali Mirchi [e]

[a] Oak Ridge Institute for Science and Education (ORISE), El Reno, OK 73036, USA
[b] USDA-Agricultural Research Service, Oklahoma and Central Plains Agricultural Research Center, El Reno, OK 73036, USA
[c] Department of Civil Engineering, Antalya Bilim University, Antalya, Turkey
[d] MEU Research Unit, Middle East University, Amman, Jordan
[e] Department of Biosystems and Agricultural Engineering, Oklahoma State University, Stillwater, OK 74078, USA

ARTICLE INFO

Keywords:
SPEI
Evapotranspiration
Probability distribution
Thornthwaite
Hargreaves
Penman-Monteith
Oklahoma

ABSTRACT

Study region: The state of Oklahoma located in the Southern Plains region of the United States.
Study focus: The standardized precipitation evapotranspiration index (SPEI) is a widely used meteorological drought index that incorporates potential evapotranspiration (PET) into a precipitation-based index. However, the understanding of the appropriate PET method for SPEI across different temporal scales in non-arid climate conditions remains limited. We compared Thornthwaite (TW), Hargreaves (HG), and Penman-Monteith (PM) equations for SPEI at various accumulations, considering three temporal scales: 1) long-term (25 years), 2) event-based, and 3) monthly. Also, we examined the log-logistic and generalized extreme value distributions to test the normality of SPEI computed from the three PET methods. To do this, we utilized high-quality climate datasets measured at 107 stations across the state of Oklahoma, United States, which has a diverse climate ranging from semi-arid to humid subtropical.
New hydrological insights for the region: The log-logistic distribution was found to be suitable for SPEI. The SPEI-HG showed better agreement with SPEI-PM than SPEI-TW in this region for the analyses of three temporal scales. However, for accumulations of SPEI longer than one year, both TW and HG equations showed no significant differences with SPEI-PM. The findings provide practical guidance for selecting an appropriate PET equation in the Southern Plains region depending on the purpose of study without resorting to data-intensive methods for PET estimation.

1. Introduction

Drought is one of the most pressing issues of our time, profoundly affecting the environment, society, and economy (Liu et al., 2021; Pyarali et al., 2022; Wilhite and Glantz, 1985). It can have detrimental effects on various sectors such as industry, agriculture, and water quality (Bussi and Whitehead, 2020; Lai et al., 2019; Rajbanshi and Das, 2021; Teutschbein et al., 2023; Wang et al., 2021). Climate change is expected to exacerbate these issues, as longer and more severe droughts are projected to become more frequent

* Corresponding author at: Oak Ridge Institute for Science and Education (ORISE), El Reno, OK 73036, USA.
E-mail address: Sanghyun.Lee@usda.gov (S. Lee).

https://doi.org/10.1016/j.ejrh.2024.101761
Received 16 August 2023; Received in revised form 8 February 2024; Accepted 27 March 2024
Available online 29 March 2024

(Ahmadalipour et al., 2017a; Li et al., 2022; Trenberth et al., 2014; Zhou et al., 2021), making it even more difficult to address the impacts of droughts in the future (AghaKouchak et al., 2021; Cook et al., 2021; Peterson et al., 2021; Saft et al., 2016). These concerns emphasize the need for more research to evaluate droughts through a rigorous approach.

Drought commonly originates from a deficiency of precipitation. Therefore, most of the meteorological drought indices utilize precipitation (Schyns et al., 2015), and these indices are usually standardized for use in drought studies (Gholizadeh et al., 2022; Johnson and Sharma, 2015; Meresa et al., 2023; Naresh Kumar et al., 2009; Tirivarombo et al., 2018; Yao et al., 2018). For example, the Standardized Precipitation Index (SPI) (McKee et al., 1993) is a key index to provide normalized anomalies in precipitation, recommended by the World Meteorological Organization (WMO, 2006). However, the SPI does not account for the effects of temperature on drought (Beguería et al., 2014; Guttman, 1998), despite several studies showing the significant role of temperature (Ahmadalipour et al., 2017b; Diffenbaugh et al., 2015; Williams et al., 2015). To address this limitation, the Standardized Precipitation Evapotranspiration Index (SPEI) was developed by Vicente-Serrano et al. (2010).

The SPEI is a variant of the SPI that incorporates the effects of temperature on drought by considering potential evapotranspiration (PET). This standardized index provides a more comprehensive assessment of drought, maintaining the simplicity, multi-temporal perspective of the SPI, making it a useful index for drought monitoring and management (Stagge et al., 2014; Strzepek et al., 2010). The SPEI uses the concept of monthly climatic water balance, which is the difference between precipitation (P) and PET. This concept compares the water availability with the atmospheric evaporative demand, providing an additional information incorporating the effects of temperature (Stagge et al., 2014).

Vicente-Serano et al. (2010) suggested the use of the Thornthwaite (TW) equation (Thornthwaite, 1948) to estimate PET for SPEI as it only requires mean air temperature and mean daylight hours, which can be calculated from latitude. However, the TW equation is based on an empirical relation between the mean temperature and PET, resulting in an underestimation of PET in arid and semiarid regions (Jensen and Allen, 2016), and an overestimation of PET in humid and tropical regions (Van Der Schrier et al., 2011). Food and Agriculture Organization of the United Nations (FAO) and the American Society of Civil Engineers (ASCE) recommended the standardized Penman-Monteith (PM; Monteith, 1965) equation for estimating PET (Allen et al., 1998; Walter et al., 2004). The PM equation incorporates physiological and aerodynamic parameters and has been validated in various climatic regions using lysimeter measurements (Berti et al., 2014). However, the PM equation requires extensive meteorological datasets (e.g., solar radiation, wind speed, relative humidity) that may not be available in many parts of the world. The Hargreaves (HG) equation that uses the maximum and minimum temperature (Hargreaves and Samani, 1985) can be an alternative method. However, the PET estimates based on HG equation also showed a range of discrepancies compared with the PM equation in different parts of the world (Amatya et al., 1995; Temesgen et al., 2005; Trajkovic, 2007).

The calculation of SPEI depends mainly on two key aspects: the choice of the probability distribution and the PET method. Previous studies examined these two aspects separately with confined climatic zones or limited datasets. These inherent constraints within previous studies imposed some hindrances on the generalization. In previous studies, various probability distributions such as log-logistic, general extreme value (GEV), log-normal, and Pearson type III were tested for SPEI. Vicente-Serrano et al. (2010) selected the log-logistic distribution for SPEI computed by TW equation based on the data at 11 stations across the world, while Stagge et al. (2015) suggested the GEV distribution as the most suited distribution for SPEI computed by PM using the watch forcing dataset (WFD) in Europe. In response to Stagge et al. (2015), Vicente-Serrano and Beguería (2016) conducted further research and tested the goodness-of-fit for different distributions based on global monthly precipitation and PET data, and recommended the log-logistic distribution for SPEI calculated from PM. Therefore, further research is needed to pinpoint the most appropriate probability distribution for SPEI for specific regional contexts.

For the choice of the PET method, even though previous studies showed that the choice of PET equation has a significant impact on the SPEI (Beguería et al., 2014; Ortiz-Gómez et al., 2022; Stagge et al., 2014), different PET equation was recommended depending on the geographic regions and climate conditions (Ortiz-Gómez et al., 2022; Zarei and Mahmoudi, 2020). Especially, these studies focused mainly on arid to semi-arid regions with limited number of stations. Further, both Beguería et al. (2014) and Stagge et al. (2014) focused simply on the correlation between SPEI series using different PET methods but did not consider the drought events and associated properties extracted from the SPEI, which is of particular interest in drought studies. In addition, Stagge et al. (2014) focused only on a 6-month accumulation period for the PET selection. However, drought is considered as a multi-temporal scale phenomenon. In other words, time scales of the response of various sources of accessible water (e.g., climatic water deficit, soil moisture, streamflow, groundwater) to precipitation deficit are different, which can cause different types of droughts (e.g., meteorological, agricultural, hydrological droughts) (Lloyd-Hughes and Saunders, 2002). Therefore, more wholistic and systematic research is imperative to consider the selection of both probability distribution and PET in various climatic conditions, especially in non-arid regions.

The main objective of this paper was to conduct a comprehensive analysis of the sensitivity of SPEI to different probability distributions and PET methods, considering TW, HG, and PM equations using 107 stations across the state of Oklahoma, where diverse climate conditions are present. We examined the log-logistic and GEV distributions to select an appropriate distribution to calculate SPEI in this region. To do this, the rejection rates based on the Shapiro-Wilks (S-W) test were compared to test normality of the SPEI computed from each PET method across various accumulation periods. For sensitivity of the SPEI to the three PET methods, three temporal scales were examined: 1) long-term (25 years), 2) event-based, and 3) monthly drought analyses at varying accumulation periods (i.e., 1–24 months). Lastly, a historical drought event was selected to facilitate a robust evaluation among the three PET methods, providing a more wholistic and systematic approach to assessing the impact of PET method selection on SPEI across Oklahoma.

2. Methods

2.1. Study area

The state of Oklahoma is in the Southern Great Plains region of the United States. Oklahoma has experienced frequent and recurring periods of droughts (Basara et al., 2013; Christian et al., 2015; Garbrecht et al., 2006), with the 1998 drought alone resulting in approximately $2.0 billion in agricultural losses (Tian and Quiring, 2019). Oklahoma has various climate conditions, ranging from humid subtropical in the east to semi-arid in the west (Fig. 1a), with a pronounced precipitation gradient from east to west (Fig. 1c). Further, temperatures decrease from south to north (Fig. 1b), while elevation increases from east to west (Fig. 1d). Given these varied climatic and topographic features, Oklahoma provides an ideal location for studying the impacts of PET on drought assessments based on the SPEI, with densely installed high-quality station-based data.

2.2. Dataset

The study utilized data from the Oklahoma Mesonet (hereafter Mesonet), an automated network of 121 stations (Brock et al., 1995; McPherson et al., 2007) reporting daily precipitation, maximum and minimum air temperature, average air temperature, and estimated potential evapotranspiration based on the Penman-Monteith equation. We used 107 active Mesonet stations that have continuous records of precipitation and temperature between 1998 and 2022, excluding any stations with missing data (Fig. 1a). Automated and manual quality assurance methods were implemented across the Mesonet stations to identify and correct sensor drift and bias as necessary (Brock et al., 1995; McPherson et al., 2007). In this study, these high-quality daily measurements were aggregated into monthly values using Python.

2.3. Potential evapotranspiration

To estimate monthly PET values, we used three PET equations: PM, TW, and HG equations. For PET based on PM (PET_{PM}), the Mesonet provides estimated daily PET data based on the ASCE Standardized reference equation (Walter et al., 2004) as follows:

$$PET_{PM} = \frac{0.408\Delta(R_n - G) + \gamma \frac{900}{T+273} u_2 (e_s - e_a)}{\Delta + \gamma(1 + 0.34u_2)} \quad (1)$$

where R_n is the calculated net radiation at the crop surface (MJ m^{-2}), G is the soil heat flux density at the soil surface (MJ m^{-2} d^{-1}), T is the mean daily air temperature at 1.5–2.5-m height (°C), u_2 is the mean daily wind speed at 2-m height (m s^{-1}), e_s is the saturation vapor pressure at 1.5–2.5-m height (kPa), Δ is the slope of the saturation vapor pressure-temperature curve (kPa $°C^{-1}$), and γ is the psychrometric constant (kPa $°C^{-1}$).

The daily PET_{PM} values were aggregated to monthly values to calculate monthly climatic water balance. Also, from monthly temperature data, PET based on Thornthwaite (PET_{TW}) and Hargreaves (PET_{HG}) were calculated using the PyETo package in Python as follows:

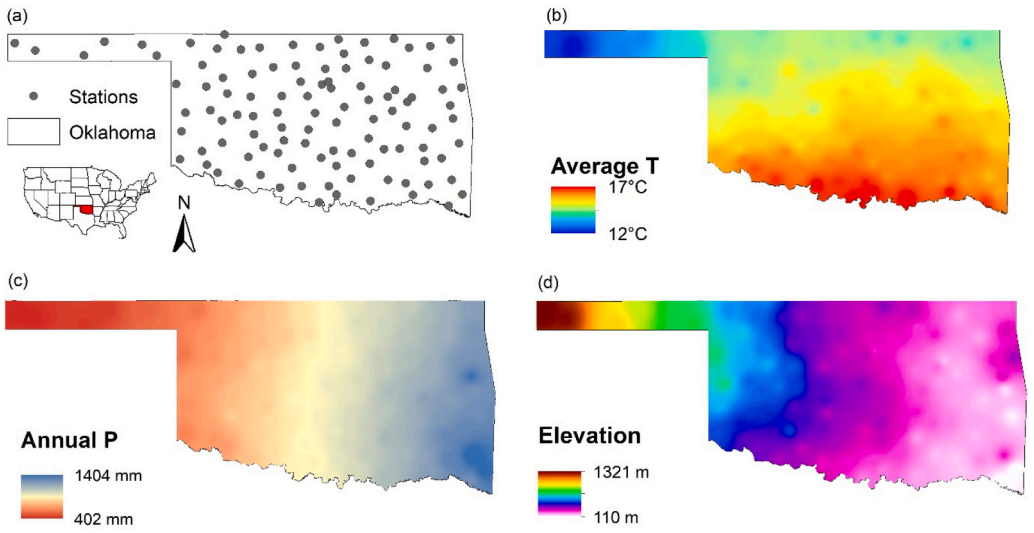

Fig. 1. Maps of (a) Mesonet stations across the state of Oklahoma with Köppen–Geiger climate classification, (b) average temperature (degree Celsius) from 1998 to 2022, (c) annual precipitation (millimeters) from 1998 to 2022, and (d) elevation (meters above mean sea level) across Oklahoma.

$$PET_{TW} = 16K\left(\frac{10T}{I}\right)^{m} \tag{2}$$

where I is the heat index for the whole year, and m is a coefficient as a function of I such that $m = 6.75 \times 10^{-7} I^3 - 7.71 \times 10^{-5} I^2 + 1.79 \times 10^{-2} I + 0.492$, and K is a correction coefficient as a function of the latitude and month.

$$PET_{HG} = 0.0023 R_a (T + 17.8)(T_{\max} - T_{\min})^{0.5} \tag{3}$$

where $T_{\max}$ and $T_{\min}$ are the maximum and minimum air temperature (°C), respectively, and R_a is extraterrestrial radiation (MJ m^{-2}).

2.4. SPEI

To estimate the SPEI values, the monthly deficit (D) should be calculated. Here, we used three different equations for PET values as discussed in Section 2.3.

$$D_i = P_i - PET_i \tag{4}$$

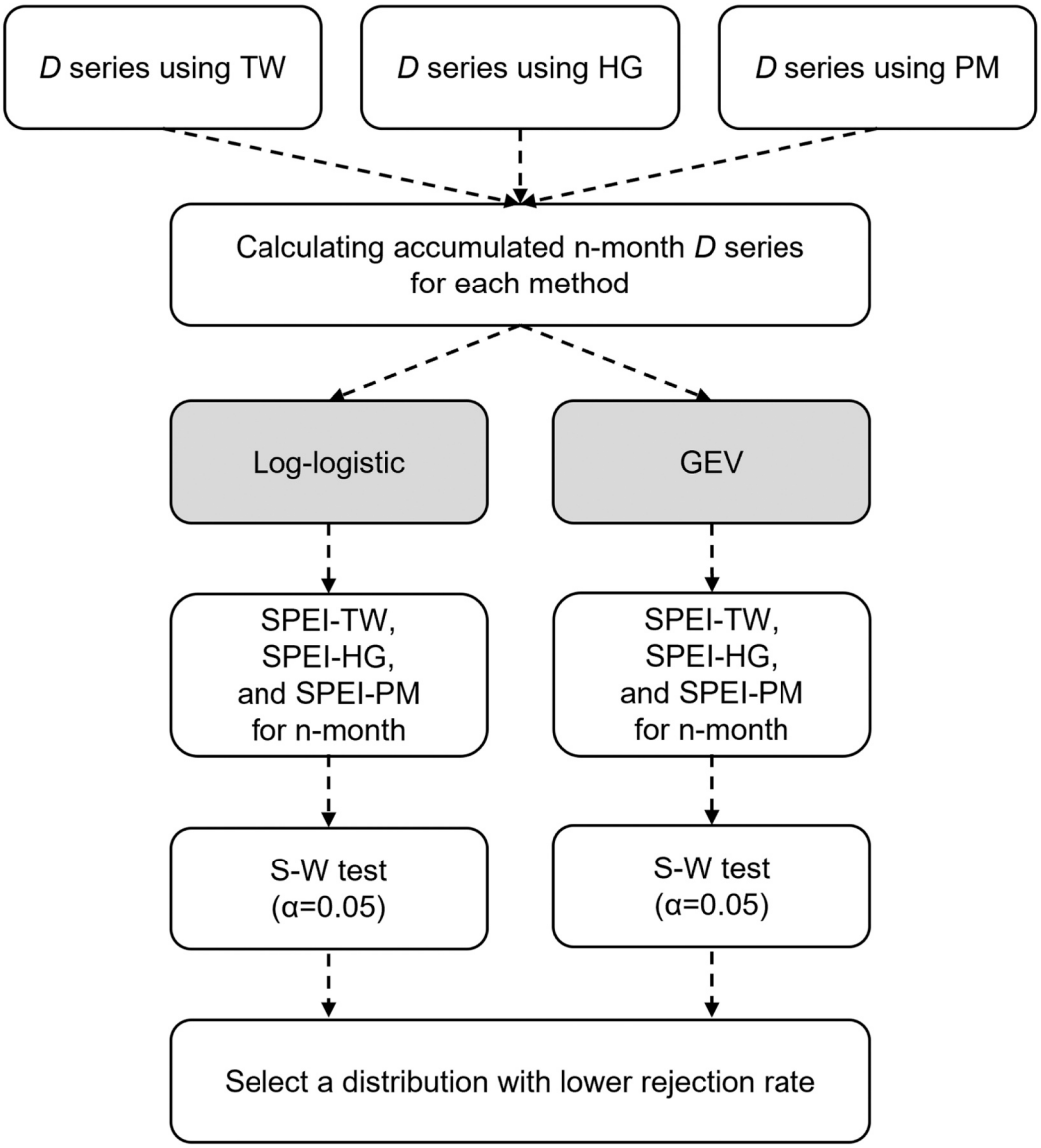

Fig. 2. Conceptual Flowchart for Selecting Probability Distribution using the Shapiro-Wilk (S-W) Test. *D* represents the monthly deficit between precipitation and PET.

Once the D_i values are calculated, the values are aggregated at different time scales. The probability distribution (e.g., three-parameter log-logistic distribution) is fitted to accumulated D_i series at each Mesonet station. Hereafter, SPEI-n represents SPEI with n-month accumulation period. The SPEI values can be calculated by standardizing the cumulative D series as follows:

$$SPEI_i = W_i - \frac{2.515517 + 0.802853W_i + 0.010328W_i^2}{1 + 1.432788W_i + 0.189269W_i^2 + 0.001308W_i^3} \quad (5)$$

$$W_i = \sqrt{-2\ln p} \text{for} p \leq 0.5 \quad (6)$$

$$W_i = \sqrt{-2\ln(1-p)} \text{for} p > 0.5 \quad (7)$$

where p is the probability of exceeding a given D_i, and the sign of the resultant SPEI is reversed for $p > 0.5$. A detailed description of calculating the SPEI is provided by Vicente-Serrano et al. (2010).

2.5. Distribution for SPEI

We evaluated the goodness-of-fit for both log-logistic and GEV distributions in fitting SPEI using ground-based datasets across Oklahoma. The resultant SPEI values represent the D series as standard normal scores with zero mean and unit variance. We followed the previous studies of Stagge et al. (2015) and Vicente-Serrano and Beguería (2016), and evaluated SPEI goodness-of-fit based on the S-W test for normality of the SPEI values. We selected the log-logistic and GEV distributions for evaluation because they generally performed better than other distributions in previous studies (Stagge et al., 2015; Vicente-Serrano et al., 2010; Vicente-Serrano and Beguería, 2016). Hence, we applied the S-W test with a significance level of α=0.05 for the SPEI fitted by the log-logistic and GEV with TW equation (SPEI-TW), HG equation (SPEI-HG), and PM equation (SPEI-PM) on different accumulation periods at the stations (Fig. 2). The parameters for each distribution were estimated using a maximum likelihood algorithm, and the rejection rate was calculated as the proportion of rejected distributions across 107 stations for each accumulation period.

2.6. Three temporal scales

In this study, we evaluated SPEI calculated by the three PET methods across three different temporal scales: long-term, event-based, and monthly drought analyses. For long-term analysis, we examined the overall relationships and disparities between the two SPEI series using the entire time series. Previous studies focused mainly on the long-term analysis using the correlation coefficient to evaluate the sensitivity of SPEI to the PET equations. However, relying only on this coefficient may lead to false conclusion, given its focus on linear relationships and susceptibility to the influence of extreme values (outliers). Especially, in drought studies, the main focus lies on drought characteristics (e.g., frequency, duration, severity) associated only with negative values of SPEI. Therefore, a More effective and practical evaluation can be achieved by directly comparing these characteristics. To address this, we conducted two additional temporal scales in this study: event-based and monthly drought analyses, enabling a more systematic approach.

2.7. Long-term drought analysis

We compared the SPEI-TW, SPEI-HG, and SPEI-PM time series using two metrics: the Pearson's correlation coefficient (r) and the mean absolute difference (MAD). To do this, the SPEI values from 1998 to 2022 were calculated at each station at different accumulation periods. Given that the PM equation has been shown to provide more realistic estimates of PET in various climate zones (Gui et al., 2021; Sheffield et al., 2012; Trenberth et al., 2013), we mainly focused on comparing the Pearson's r and MAD between the SPEI-PM and the other two series to determine which one provides closer results for the SPEI series. Note that the statistical analyses in this study were performed using the SciPy library in python.

2.8. Event-based drought analysis

For the event-based drought analysis, we quantified drought characteristics (e.g., drought frequency, duration, severity, and intensity) from the SPEI series. Drought can be classified into three classes: moderate, severe, and extreme with the corresponding SPEI

Table 1
Classifications of drought using SPEI indices (Danandeh Mehr et al., 2020).

Classification	*SPEI threshold (Log-logistic)*
Extremely wet	1.83 ≤ SPEI
Severely wet	1.82 < SPEI < 1.43
Moderately wet	1.42 < SPEI < −1.0
Near normal	-1.0 ≤ SPEI ≤ 1.0
Moderate drought (MoD)	-1.42 < SPEI < −1.0
Severe drought (SD)	-1.82 < SPEI < −1.43
Extreme drought (ED)	SPEI ≤ −1.83

value ranges of −1.42 to −1.0, −1.82 to −1.43, and ≤ −1.83, respectively (Table 1) (Danandeh Mehr et al., 2020). Here, we defined a drought event as the SPEI values less than −1.43, which corresponded to severe drought (Table 1). Using this threshold value, drought frequency was defined as the number of drought events, while drought duration was defined as the number of consecutive months associated with each event. The drought severity was calculated as the cumulative sum of the SPEI values in each event, and the intensity was determined as the ratio of severity to duration for the corresponding event. We extracted the maximum duration and median severity and intensity for each station from 1998 to 2022 following Chiang et al. (2021).

To determine whether each drought characteristic extracted from the three SPEI series (i.e., SPEI-TW, SPEI-HG, and SPEI-PM) at 107 stations behaves differently, we estimated the probability density function (PDF) for each drought characteristic using Kernel density estimation (KDE) and conducted a two samples Kolmogorov-Smirnov (K-S) test for each PDF. Note that the KDE and K-S test were performed using the SciPy library in Python.

2.9. Monthly drought analysis

We used the drought classifications presented in Table 1 to identify and quantify the occurrences of moderate drought (MoD), severe drought (SD), and extreme drought (ED) for accumulation periods ranging from 1-24 months at 107 stations between 1998 and 2022. Specifically, we counted the number of months that the SPEI values fell below each threshold value for MoD, SD, and ED, based on the three different PET methods: SPEI-TW, SPEI-HG, and SPEI-PM. This allowed us to examine how the choice of PET method influenced the number of detected drought months. To determine whether there were statistically significant differences between the counted months for each SPEI classification, we performed a Mann-Whitney U test (α=0.05) (Mann and Whitney, 1947), which can be used to compare two independent samples, on the respective counted months that resulted from 107 stations.

2.10. Comparison with a historical drought event

For the assessment endpoint, we selected one of the most severe historical droughts that occurred in 2011 across Oklahoma. This analysis involved a comparison with the SPEI-3 values computed using three PET methods (i.e., SPEI-TW, SPEI-HG and SPEI-PM). To establish a benchmark, we downloaded the U.S. Drought Monitor map in October 2011 from the Map Archive (https://

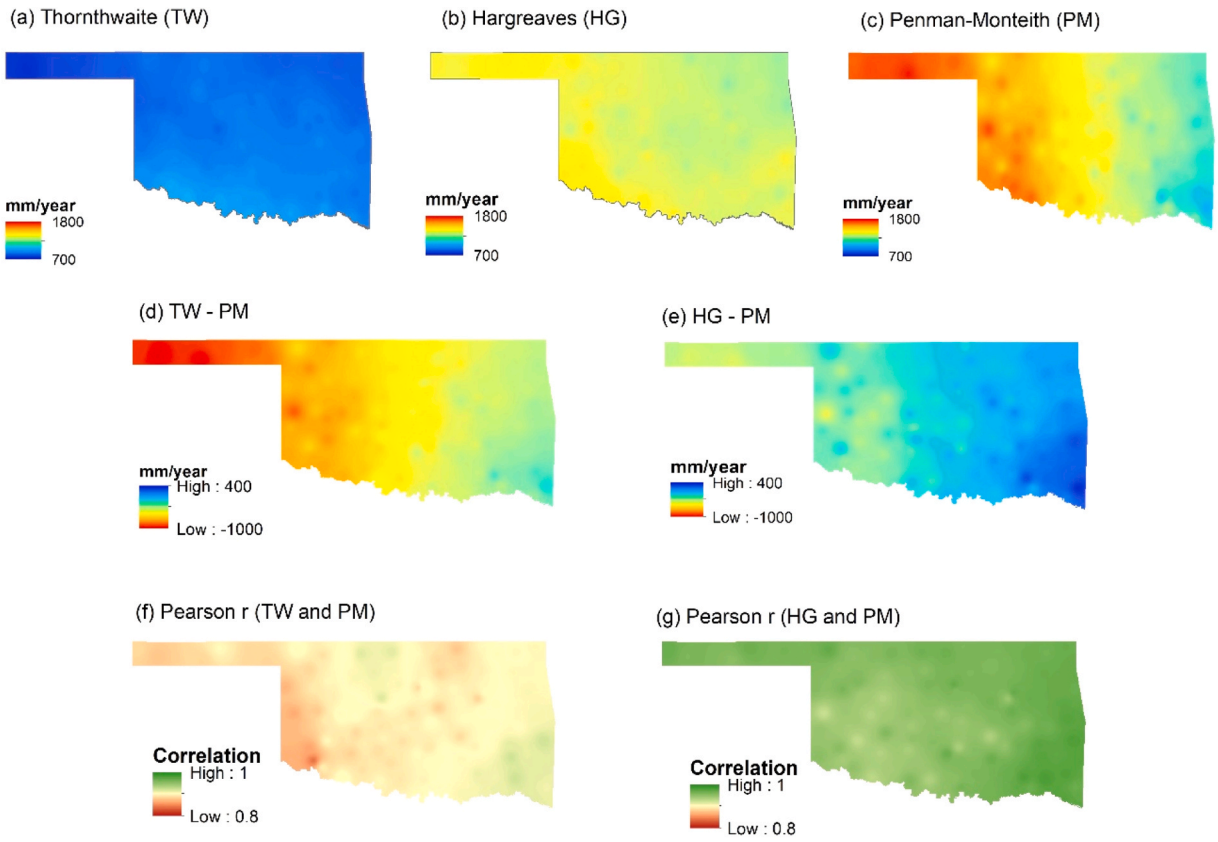

Fig. 3. Spatial distribution of estimated annual average potential evapotranspiration (PET) based on (a) Thornthwaite (TW), (b) Hargreaves (HG), and (c) Penman-Monteith (PM) methods, and the differences in annual average values between (d) TW and PM, (e) HG and PM, and the Pearson's *r* between (f) TW and PM, and (g) HG and PW across Oklahoma.

droughtmonitor.unl.edu/Maps/MapArchive.aspx). This map classified drought intensity into five levels, ranging from D0 to D4, with D4 representing the most severe drought. To align SPEI values with the U.S. Drought Monitor map, we classified SPEI values based on Table 1. For instance, we assumed that D4 in the U.S. Drought Monitor corresponds to "Extreme Drought" in Table 1. Using this method, we compared the percentage area of each category to provide a more comprehensive evaluation of the SPEI calculated from the three PET methods.

3. Results

3.1. Potential evapotranspiration

The monthly PET was calculated using TW, HG, and PM methods at 107 Mesonet stations across Oklahoma (Figure S1). The spatial distribution of annual PET values showed different patterns (Fig. 3a-c). The PM resulted in a large variation in PET, with values ranging from 990 to 1800 mm/year across Oklahoma, while the PET values ranged from 730 to 980 mm/year and from 1200 to 1500 mm/year for TW and HG, respectively. Despite the significant spatial variability in PET estimated with PM, TW and HG demonstrated relatively uniform spatial distributions. Specifically, TW and HG showed approximately 190 and 300 mm/year of variability, respectively, whereas PM showed a much broader range of 800 mm/year across different climates. This result underscores the robustness and reliability of the PM method for estimating PET, highlighting potential limitations inherent in both TW and HG methods. On average, the HG equation produced the PET values lying between the TW and PM (Fig. 3a-c). The TW equation underestimated PET compared to the PM methods, except for the east parts of Oklahoma (Fig. 3d), due in part to the assumption of zero PET below freezing temperatures (Stagge et al., 2014). Especially, the TW method significantly underestimated PET values in semi-arid region, which aligned with the previous findings of Jensen and Allen (2016). The HG method overestimated PET values in the humid subtropical region, while showing relatively less discrepancies in the semi-arid area compared to PM method (Fig. 3e). A higher correlation was observed between monthly PET_{Hg} and PET_{PM} across the entire Oklahoma (Fig. 3g), while the correlation between monthly PET_{Th} and PET_{PM} ranged from 0.84 to 0.92 (Fig. 3f), based on the Pearson's r.

3.2. Distribution for SPEI

The rejection rates based on the S-W test for both distributions were below 5% for all accumulation periods (Fig. 4). The log-logistic distribution performed better when using the TW equation for SPEI (Fig. 4a) except for SPEI-1, while the GEV distribution showed lower rejection rates for 1-, 2-, and 3-month accumulations, with SPEI-HG (Fig. 4b). However, for SPEI-PM, which is considered to provide the most realistic estimates of PET, the log-logistic distribution exhibited lower rejection rates than the GEV distribution, except for the 24-month accumulation period (Fig. 4c). In addition, the log-logistic distribution demonstrated lower or similar rejection rates in terms of the mean values for all accumulation periods compared to the GEV distribution (Table 1). Therefore, based on these results, we selected the log-logistic distribution to fit the D series for SPEI.

3.3. Long-term drought analysis

The Pearson's r was computed separately for the three different SPEI series at 107 locations across various accumulation periods (Fig. 5). The highest correlation was observed between SPEI-TW and SPEI-HG, which were computed from minimal-data PET equations, for all accumulations (indicated as TW-HG in Fig. 5). However, since our focus is on comparisons of the SPEI series resulting from minimal-data equations (i.e., TW and HG) with the data-intensive equation (i.e., PM equation), we closely examined the comparisons between TW-PM, and HG-PM. Among the two series, we found that the SPEI-HG showed a higher correlation with SPEI-PM compared to the correlation between SPEI-TW and SPEI-PM (i.e., TW-PM in Fig. 5), which showed the weakest correlations across all timescales (Fig. 5).

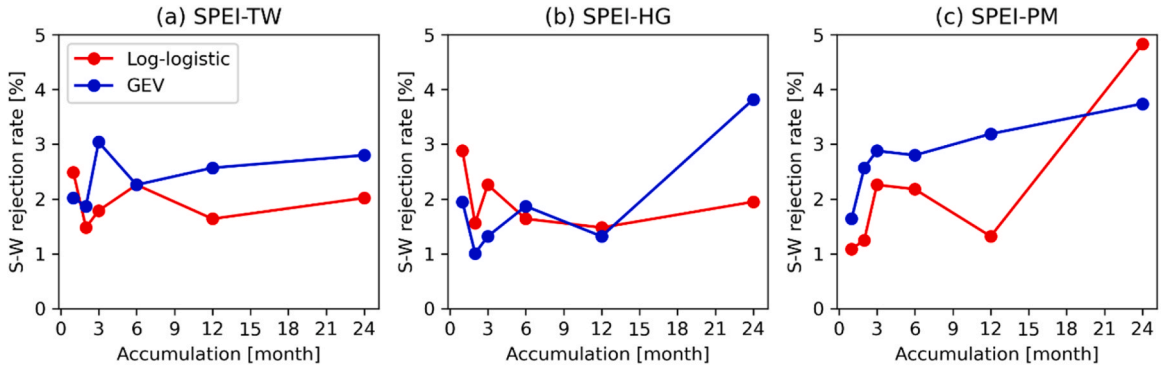

Fig. 4. Shapiro-Wilk rejection frequency (%) for SPEI distributions using (a) Thornthwaite, (b) Hargreaves, and (c) Penman-Monteith methods across different accumulation periods.

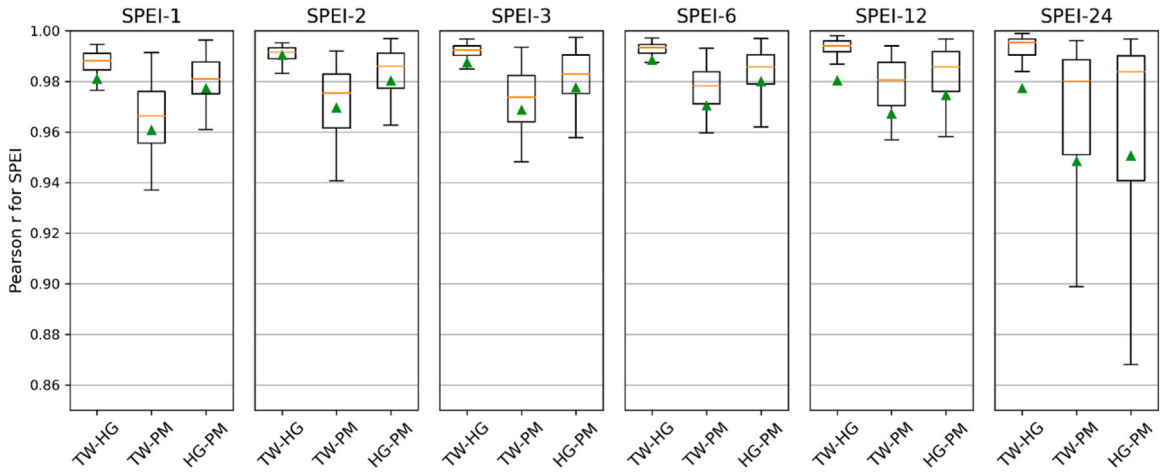

Fig. 5. Pearson's *r* between SPEI series calculated by Thornthwaite (TW), Hargreaves (HG), and Penman-Monteith (PM) equations at 107 Mesonet stations. TW-HG represents the correlations between SPEI-TW and SPEI-HG. The green triangle represents the mean value, and each box plot shows the minimum, first quartile, median (orange line), third quartile, and maximum.

Since the highest variations in the coefficients were observed for the 24-month accumulation period while the other periods remained almost constant variations for TW-PM and HG-PM (Fig. 5), we further examined the spatial pattern of the correlation for SPEI-1 and SPEI-24 (Fig. 6). In general, the correlations between HG-PM showed consistently higher values across Oklahoma compared with TW-PM. For both TW-PM and HG-PM, however, we found relatively higher correlations in the humid climate region (i.e., the eastern parts of Oklahoma) regardless of temporal scales (Fig. 6). However, for 24-month accumulations, both TW-PM and HG-PM produced relatively lower correlations in the semi-arid region (i.e., the western parts of Oklahoma) (Figs. 6c and 6d). The longer accumulations tend to smooth seasonal fluctuations and intra-annual variability, and this long-term averaging effect may exacerbate the discrepancies arising from the choice of PET methods, particularly in drier regions (Fig. 6c and d). Consequently, these discrepancies resulted in higher variations of the correlation compared to other short-term accumulations (Fig. 5). These results were

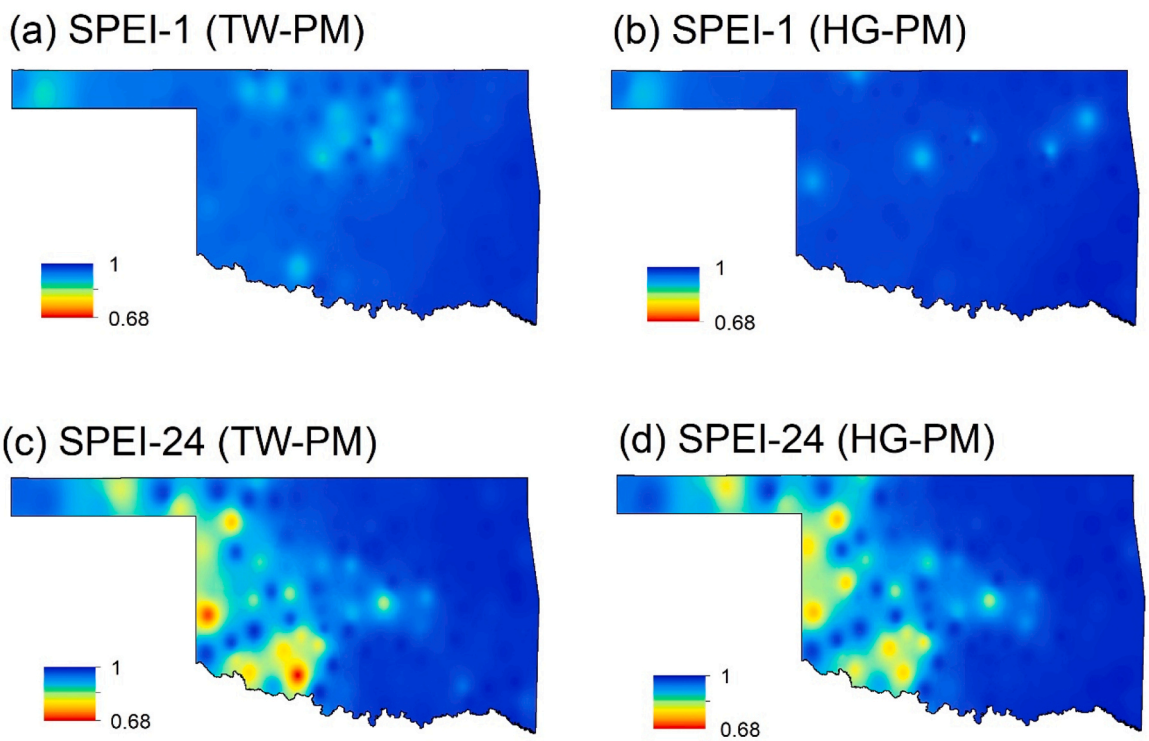

Fig. 6. Spatial distribution of Pearson's *r* between (a) SPEI-TW and SPEI-PM, (b) SPEI-HG and SPEI-PM for 1-month accumulation, and (c) SPEI-TW and SPEI-PM, (d) SPEI-HG and SPEI-PM for 24-month accumulation.

associated with the results of PET discussed in the Section 3.1, aligned with the findings of Beguería et al. (2014) that the selection of PET methods for SPEI is relatively non-significant in areas with high precipitation and vice versa for longer periods.

To confirm this conclusion, we examined the relationships between the correlations of the SPEI series (i.e., Pearson' *r* of SPEI-12) with annual average precipitation and temperature across the Mesonet stations using the non-parametric Spearman's Rho coefficient (Figure S2). The results showed that the Pearson' *r* between the SPEI series had strong positive correlations with annual precipitation. In other words, the choice of different PET methods is non-significant in humid regions as both SPEI-TW and SPEI-HG showed very high correlations with SPEI-PM. However, there were no significant relationships with the annual mean temperature (Figure S2).

In terms of the differences in the SPEI values, the smallest difference was observed from TW-HG. However, when compared to SPEI-PM, SPEI-HG showed less difference than SPEI-TW with the SPEI-PM for all accumulated months (Fig. 7). Therefore, the SPEI computed from the HG equation showed a closer behavior with the SPEI-PM than the SPEI-TW in diverse climate conditions across various temporal scales. This suggests that the HG equation may be a useful alternative to the PM method when considering long-term SPEI.

3.4. Event-based drought analysis

The KDE of drought characteristics (i.e., frequency, duration, severity, and intensity) were calculated from the SPEI-TW, SPEI-HG, and SPEI-PM for various accumulations between 1998 and 2022. Overall, for shorter accumulations (up to 6-month), the KDE of SPEI-HG fell between that of the SPEI-TW and SPEI-PM in most cases. For the 6-month accumulation, for example, the peak of SPEI-HG for the frequency, maximum duration, and intensity were closer to SPEI-PM compared to SPEI-TW (Fig. 8). In contrast, for longer accumulations (e.g., 12- and 24-month), there were no significant differences in the KDE of drought characteristics between the three PET methods. For 24-month, the KDE of SPEI-HG and SPEI-PM showed almost identical behaviors, while the KDE for intensity from all three methods was virtually indistinguishable (Fig. 9). In addition to KDE, the spatial patterns of drought characteristics were also examined for shorter and longer accumulations. For example, SPEI-HG and SPEI-PM demonstrated similar spatial patterns (Fig. 10b and c), while SPEI-TW had a different pattern and range for its maximum duration (Fig. 10a) for 6-month accumulation. However, as an example of longer accumulation periods, the drought severity of SPEI-12 computed from the three equations showed relatively similar spatial patterns across Oklahoma (Figs. 10d-f). Note that the y-axis values, which is dimensionless, represent the density or the relative likelihood of observing data at a particular point on the x-axis. The values on the y-axis are relative and are scaled in a way that the total area under the curve integrates to 1 over the entire range of possible values on the x-axis.

To further examine the differences observed between shorter and longer accumulations, the two sample Kolmogorov-Smirnov (K-S) test (α=0.05) was implemented for each drought characteristic for all accumulation periods. The results confirmed that there were no differences between the drought characteristics calculated from TW, HG, and PM equations for longer accumulations (e.g., 12- and 24-months), while some differences were observed up to 6-month accumulation (Table 3). In terms of frequency and severity, both TW and HG showed significant differences with PM for most of shorter accumulations. However, for maximum duration, HG and PM constantly resulted in comparable results, while TW showed significant difference with PM for the most accumulations. Lastly, in terms of drought intensity, both TW and HG resulted in comparable results with PM, except for the 2-month accumulation. Based on the findings, we conclude that for relatively shorter accumulation periods, the use of HG equation is recommended when data is limited to PM method, while for longer accumulations, all three equations exhibited comparable results for the drought characteristics. Thus, the impacts of the choice of PET method for SPEI on drought characteristics is negligible for longer accumulation periods.

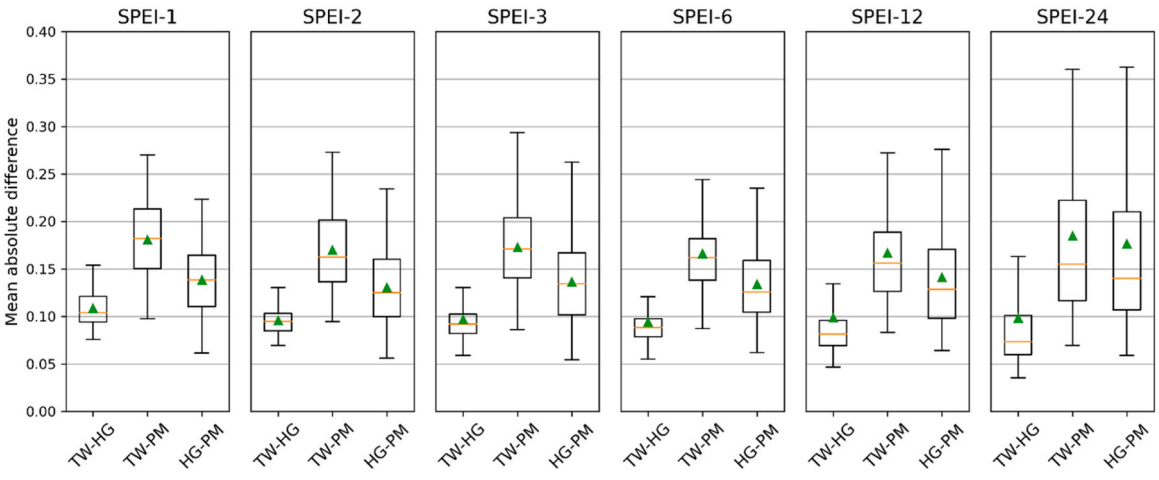

Fig. 7. Mean absolute difference (MAD) between SPEI series calculated by Thornthwaite (TW), Hargreaves (HG), and Penman-Monteith (PM) equations at 107 Mesonet stations. The green triangle represents the mean value.

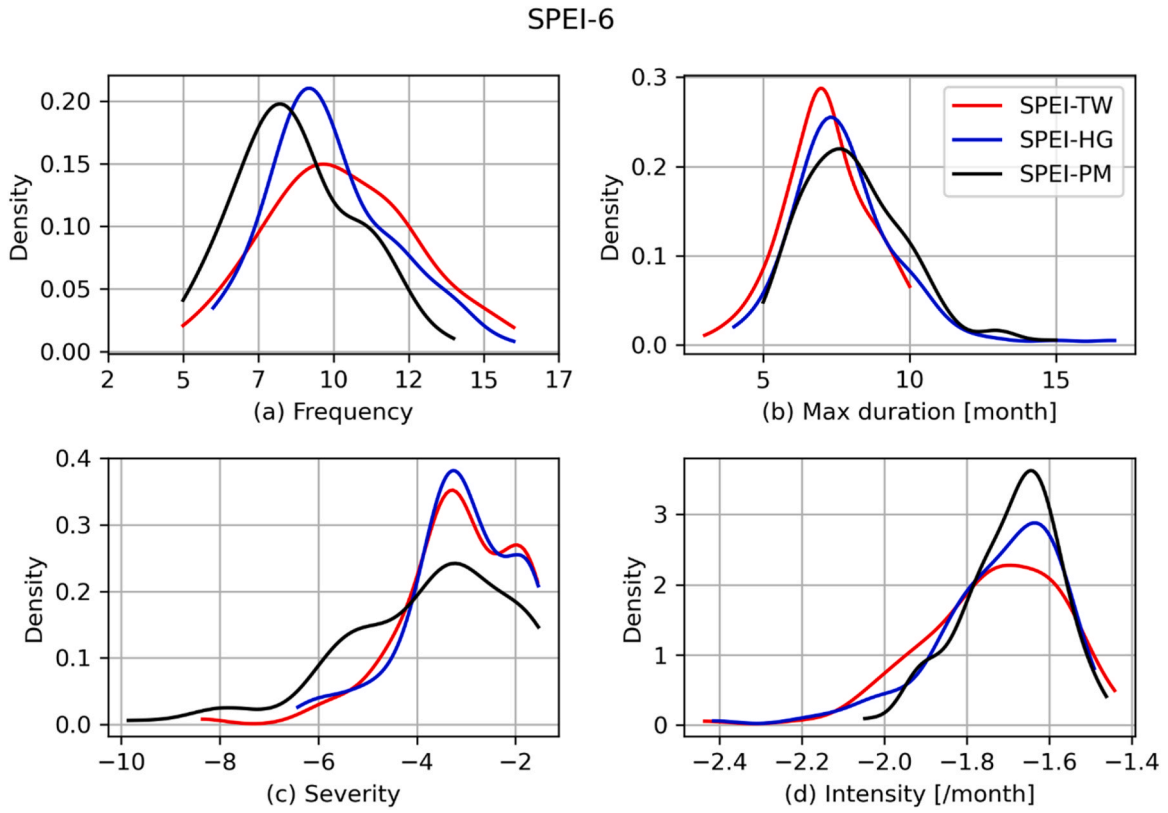

Fig. 8. Kernel density estimations for characteristics of severe drought events: (a) frequency, (b) Maximum duration, (c) Median severity, and (d) median intensity based on SPEI-6 using Thornthwaite (TW), Hargreaves (HG), and Penman-Monteith (PM) equations at 107 Mesonet stations.

3.5. Monthly drought analysis

The Mann-Whitney U test identified 6 significant differences out of 36 cases in terms of drought occurrences, while 5 differences were observed in the 1-month accumulation (Table 4). However, for the rest of the accumulation periods, SPEI-TW and SPEI-HG did not show any significant differences with SPEI-PM, except for one case (i.e., SPEI-HG and SPEI-PM at 3-month accumulation for ED) (Table 4). Especially, for longer accumulations (e.g., 6-, 12- and 24-month), both TW and HG showed no significant differences with PM in this analysis (Table 3). Therefore, depending on the interest in drought severity, the alternative parsimonious equation can be chosen.

To examine the spatial distributions of the probability of occurrences for MoD, SD, and ED drought across Oklahoma, the results based on the SPEI series from the three PET equations at a 12-month accumulation were analyzed (Fig. 11). Note that the probability of occurrence was calculated by dividing the number of months classified as drought (e.g., MoD, SD, and ED) by the total number of months in the study period. The Cohen's Kappa coefficient (κ) (McHugh, 2012) was used to measure the agreements in the spatial distributions resulting from SPEI-TW and SPEI-HG with those of SPEI-PM. This coefficient ranges between −1 and 1, where a value of 1 represents complete agreement. For MoD, SD, and ED, the SPEI-HG showed the coefficients of 0.67, 0.67, and 0.72, respectively, compared with SPEI-PM, showing consistently higher values compared to SPEI-TW (Fig. 11). Based on the visual inspections and the coefficient values, we concluded that the SPEI-HG performed better than SPEI-TW, while the use of any PET method for SPEI did not produce significant differences with SPEI-PM at longer accumulations in terms of detecting drought occurrences.

3.6. Comparison with a historical drought event

In October 2011, a significant historical drought was chosen as the benchmark for comparing SPEI-TW, SPEI-HG, and SPEI-PM against the U.S. Drought Monitor (USDM) map across Oklahoma. Based on the USDM, all regions in Oklahoma experienced at least D2 intensity, corresponding to a moderate drought in Table 1 (Fig. 12). Approximately 80% of Oklahoma experienced a minimum of D3-level drought conditions (Table 5). Among the three SPEI estimates, SPEI-PM closely matched this at 76%, while SPEI-TW reported the lowest estimate at 45% (Table 5). Except for the northeastern part, most of Oklahoma was categorized as either D3 or D4 based on the USDM map (Fig. 12d), with SPEI-PM showing a similar spatial pattern (Fig. 12c), confirming the validity of using SPEI-PM as the benchmark in this study. While both SPEI-TW and SPEI-HG underestimated the severity of the drought compared to the USDM, SPEI-HG performed slightly better than SPEI-TW in terms of both percentage area and spatial distribution (Table 5 and Fig. 12).

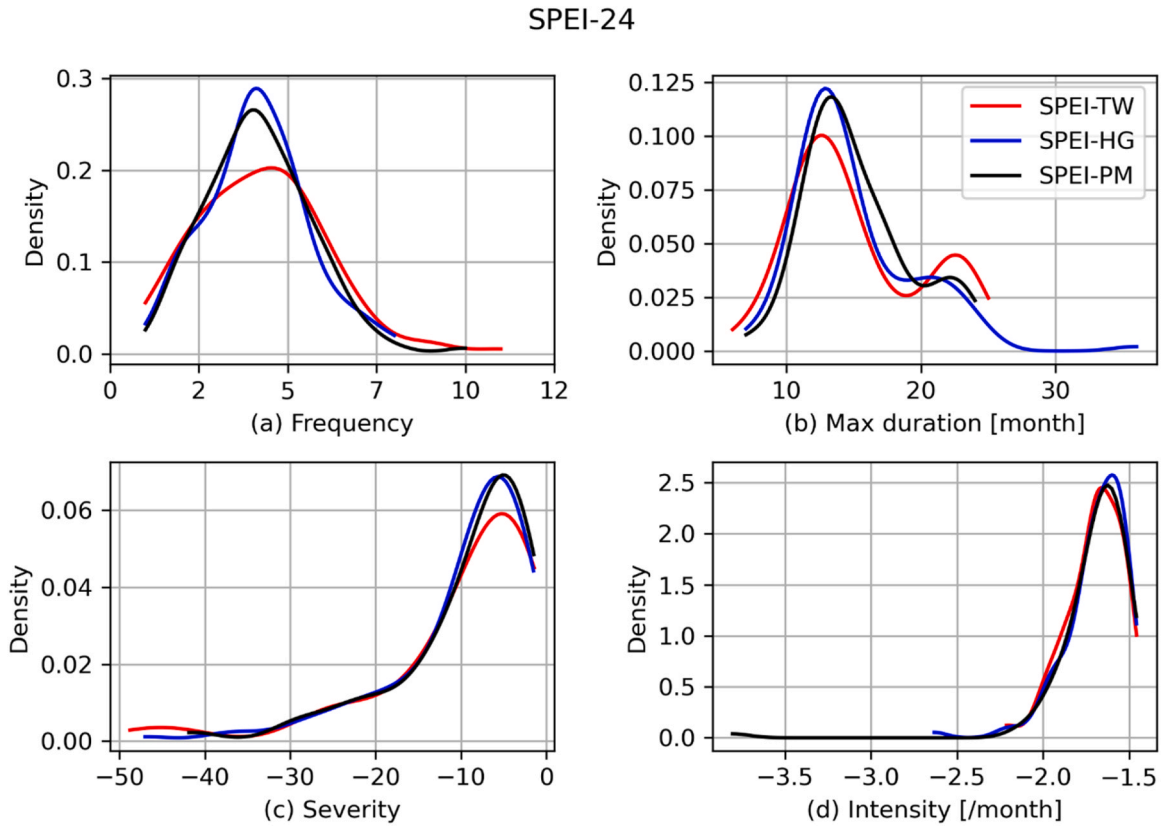

Fig. 9. Kernel density estimations for characteristics of severe drought events: (a) frequency, (b) Maximum duration, (c) Median severity, and (d) median intensity based on SPEI-24 using Thornthwaite (TW), Hargreaves (HG), and Penman-Monteith (PM) equations at 107 Mesonet stations.

4. Discussion

The presented work mainly examined the impacts of PET methods on SPEI across Oklahoma, which is dominantly in tropical climate zone. Previous studies on this subject focused mainly on arid regions (Ortiz-Gómez et al., 2022; Zarei and Mahmoudi, 2020), as the selection of a suitable PET equation for SPEI was considered less significance especially in areas receiving high precipitation (Beguería et al., 2014). This was valid only when considering the entire time series as discussed in Section 3.3 such that both SPEI-TW and SPEI-HG showed very high correlations with SPEI-PM in areas receiving high precipitation (Figure S2). However, further analysis in this research revealed noticeable differences in terms of drought events and occurrences depending on the choice of PET method (Figs. 10 and 11). For example, the SPEI-TW underestimated the area of the red region (i.e., highest probability category) for severe drought (Fig. 11) by 16% compared to SPEI-PM. These discrepancies were observed not only in semi-arid areas, but also in many parts of the subtropical areas across Oklahoma (Fig. 11). Compared with a historical drought occurred in 2011, SPEI-PM showed similar spatial patterns with the U.S. Drought Monitor map, confirming its robustness as a benchmark used in this study. Therefore, when data is available, the use of Penman-Monteith method is preferable instead of using minimal-data PET equations for SPEI calculation. Nonetheless, the findings presented in this study highlight the need for region-specific research with more comprehensive analysis at various temporal scales, rather than focusing only on long-term analysis.

Droughts are not confined to specific regions, but occur worldwide, affecting various aspects of water resources, ecosystems, agriculture, and human societies (Van Loon, 2015). Lack of water resources can affect drinking water supply, irrigation, crop failure, electricity production (hydropower or cooling water) (Van Loon, 2015). Also, freshwater ecosystems can encounter significant alterations in dissolved oxygen levels, water quality, stream connectivity, available habitat, and other essential for sustaining fish (Ramírez et al., 2018). Especially, in last decades, drought becomes a major hazard, accounting for 34% of disaster-related death worldwide (Douris et al., 2021), with cascading impacts, triggering secondary events such as wildfires and insect outbreaks (Gill and Malamud, 2014). The rising temperature due to climate change has led to intensified drought-related risks in numerous regions worldwide (Lee and Ajami, 2023; Tripathy et al., 2023). This increase significantly alters the PET rate, which holds a crucial role in determining water demand in various sectors. This underscores the necessity of identifying the suitable/alternative PET method for accurate drought predictions, which would ultimately aid in making informed decisions to mitigate the impacts of drought.

Although SPEI-HG consistently showed better agreements with SPEI-PM compared to SPEI-TW in this region, it should be noted that there are limitations associated with these minimal-data PET equations. For example, the accuracy of alternative PET equations

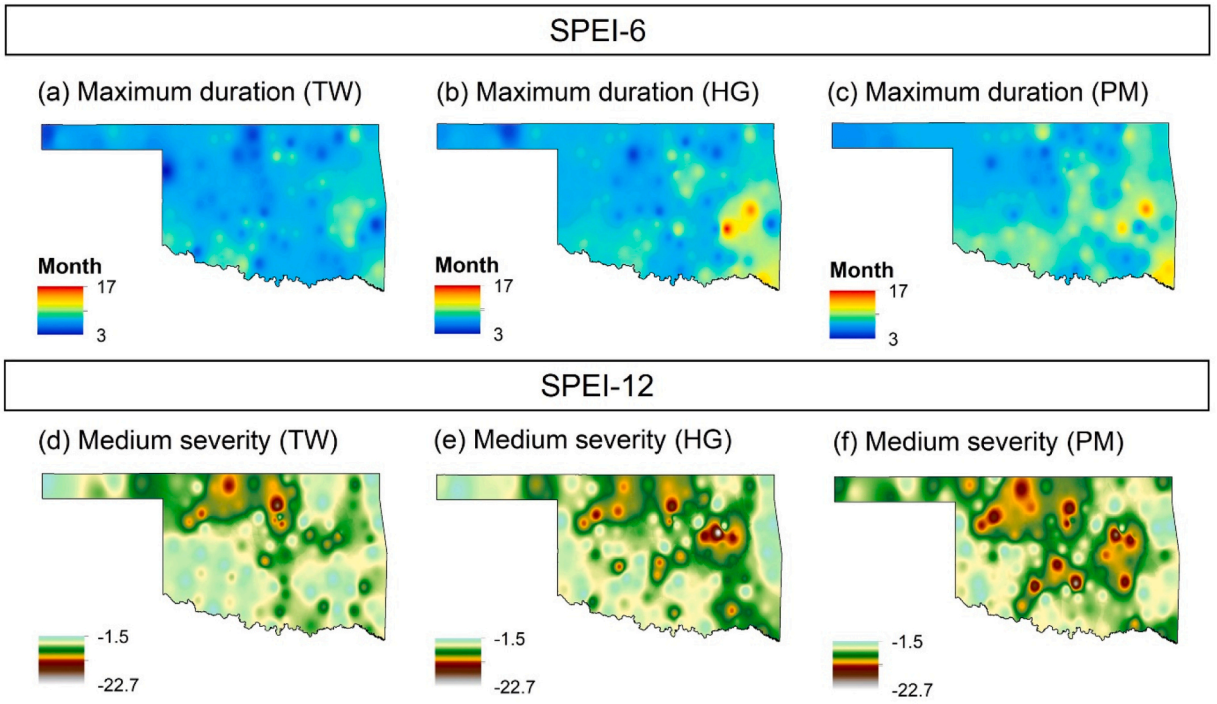

Fig. 10. Spatial distribution of maximum duration of drought events based on SPEI-6 using (a) Thornthwaite (TW), (b) Hargreaves (HG), and (c) Penman-Monteith (PM) equations, and medium severity of drought events based on SPEI-12 using (d) TW, (e) HG, and (f) PM equations across Oklahoma.

Table 2
Mean rejection rates of S-W test for all accumulation periods.

SPEI type	*Log-logistic [%]*	*GEV [%]*
SPEI-TW	1.95	2.43
SPEI-HG	1.96	1.88
SPEI-PM	2.15	2.80

Table 3
P-values of two sample Kolmogorov-Smirnov test for comparisons in drought characteristics between TW, HG, and PM methods.

Property	Comparison	1-month	2-month	3-month	6-month	12-month	24-month
Frequency	TW vs. HG	1.00	0.01	0.74	0.41	0.51	0.85
	HG vs. PM	0.00	0.00	0.00	0.00	0.51	1.00
	TW vs. PM	0.00	0.00	0.00	0.00	0.07	0.98
Max. duration	TW vs. HG	0.63	0.63	0.93	0.25	0.74	0.74
	HG vs. PM	0.01	0.07	0.63	0.63	0.51	0.74
	TW vs. PM	0.00	0.01	0.13	0.01	0.05	0.32
Median severity	TW vs. HG	0.63	0.25	0.74	1.00	0.51	0.85
	HG vs. PM	0.85	0.01	0.00	0.01	0.25	0.93
	TW vs. PM	1.00	0.00	0.01	0.01	0.13	1.00
Median intensity	TW vs. HG	0.63	0.98	0.74	0.41	0.85	0.51
	HG vs. PM	0.85	0.05	0.63	0.51	0.98	0.93
	TW vs. PM	1.00	0.01	0.25	0.07	0.25	0.41

can vary depending on the climate zone and geographic location. Although the SPEI-HG reasonably performed well in Oklahoma, this may not be the case in other regions. The minimal-data equations are often used for SPEI because of their simplicity and ease of use. However, it is recommended to carefully consider potential biased estimates of minimal-data PET to ensure the accuracy, reliability, and applicability of the research. Nonetheless, the results and findings in this study may be of great importance for drought analysis in the Southern Plains region of the United States.

Table 4
P-values of Mann Whitney U Test for comparisons in occurrence of Moderate (MoD), Severe (SD), and Extreme Droughts (ED) observed between TW, HG, and PM methods.

Property	Comparison	1-month	2-month	3-month	6-month	12-month	24-month
MoD	HG vs. PM	0.05	0.11	0.86	0.47	0.45	0.82
	TW vs. PM	0.31	0.63	0.80	0.70	0.50	0.83
SD	HG vs. PM	0.00	0.94	0.49	0.50	0.36	0.34
	TW vs. PM	0.01	0.17	0.61	0.30	0.25	0.15
ED	HG vs. PM	0.04	0.37	0.01	0.09	0.13	0.09
	TW vs. PM	0.00	0.09	0.08	0.14	0.07	0.05

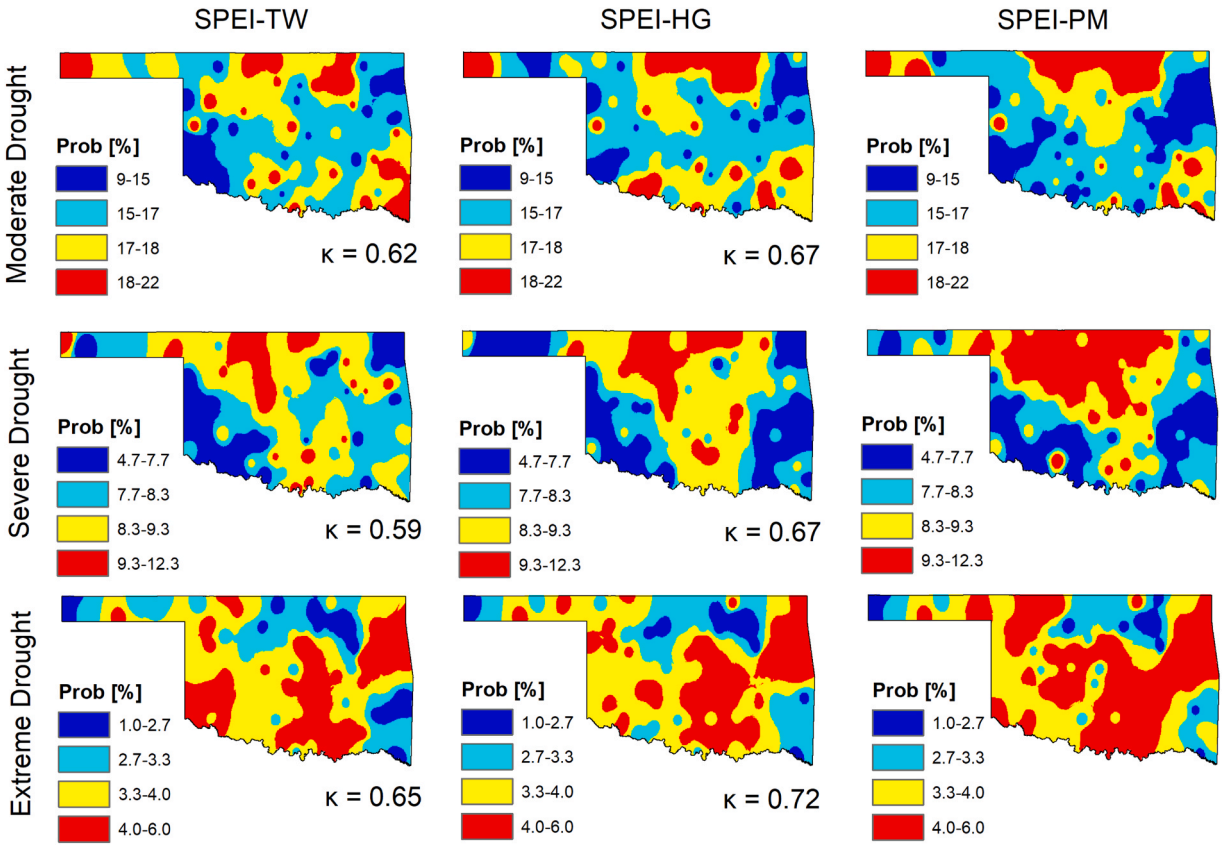

Fig. 11. Spatial distributions of the probability of occurrence [%] for Moderate, Severe, and Extreme droughts based on SPEI-12 using Thornthwaite (TW), Hargreaves (HG), and Penman-Monteith (PM) equations. The value of κ represents the Cohen's Kappa coefficient, compared to the drought detected by PM.

5. Conclusions

We analyzed the sensitivity of the SPEI for three different PET methods (TW, HG, and PM) at various accumulation periods (i.e., 1–24 months) for three temporal scales: 1) long-term, 2) event-based, and 3) monthly. Given that many parts of the world do not have the required data for the Penman-Monteith (PM) method, it is important to explore alternative minimal-data potential evapotranspiration (PET) equations that can be used for drought assessments. We considered the log-logistic and GEV distributions to evaluate the normality of SPEI. Based on the S-W test results, we selected the log-logistic distribution to fit the monthly deficit for SPEI. The long-term analysis of the SPEI revealed that overall, the SPEI-HG performed better than SPEI-TW compared with SPEI-PM. For the event-based drought analysis, SPEI-HG showed similar results to SPEI-PM, while for longer accumulations, there were no significant differences in terms of the drought characteristics (e.g., frequency, duration, severity, and intensity) extracted from the three equations. For monthly drought analysis, HG equation revealed a better alternative to PM for detecting the occurrence of moderate, severe, and extreme drought months. However, for longer accumulations, the SPEI calculated from the three equations showed no statistically significant differences for the drought analysis. Drought indices such as SPEI are commonly used for monitoring drought events or quantifying drought characteristics at various accumulation periods. Therefore, the comparison results based on the three temporal

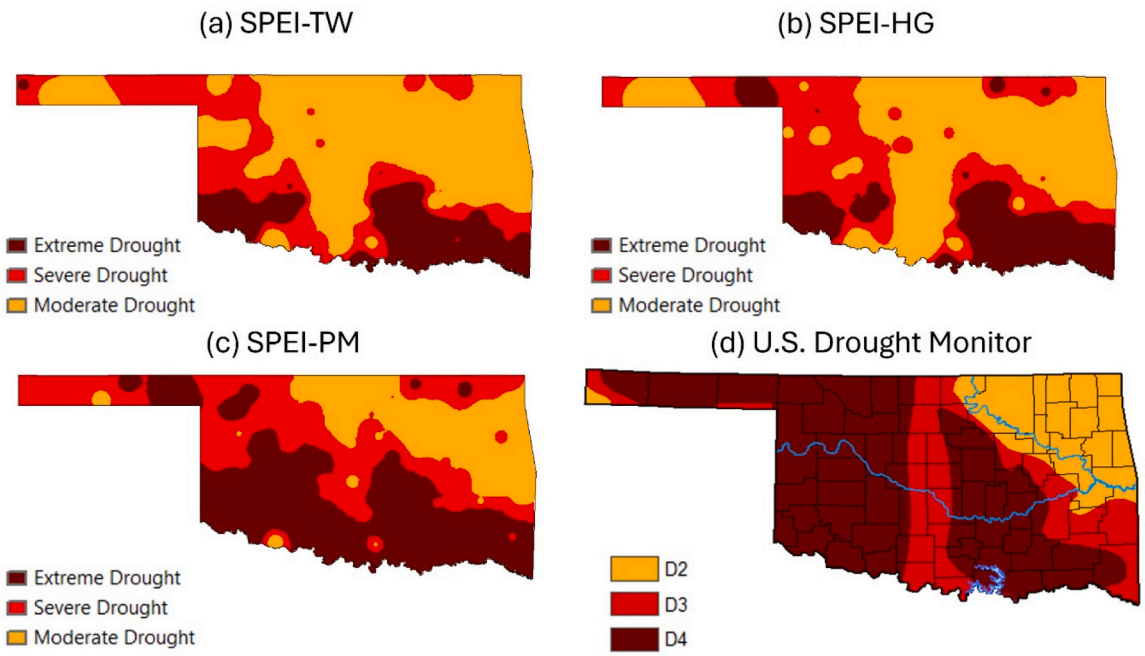

Fig. 12. Comparison of spatial distribution of drought intensity based on (a) SPEI-TW, (b) SPEI-HG, and (c) SPEI-PM, and (d) U.S. Drought Monitor map in October 2011. The U.S. Drought Monitor map was downloaded at https://droughtmonitor.unl.edu/Maps/MapArchive.aspx.

Table 5
Percentage area of drought intensity in October 2011 across Oklahoma.

Drought Intensity	SPEI-TW	SPEI-HG	SPEI-PM	US Drought Monitor
Moderate Drought (D2)	55	48	24	20
Severe Drought (D3)	26	31	33	21
Extreme Drought (D4)	19	22	42	59

Note: Moderate, severe, extreme droughts for SPEI are based on Table 1, while D2, D3, D4 represent drought intensities for the US Drought Monitor map

scales at various accumulation periods can provide more practical guidance when choosing a minimal-data PET method for computing SPEI. The results indicated that depending on the purpose of study, an appropriate method for PET can be chosen where data is scarce and uncertain for PM method.

CRediT authorship contribution statement

Ali Danandeh Mehr: Writing – review & editing, Supervision, Conceptualization. **Ali Mirchi:** Writing – review & editing, Supervision, Funding acquisition. **Sanghyun Lee:** Writing – review & editing, Writing – original draft, Validation, Software, Methodology, Investigation, Formal analysis, Data curation, Conceptualization. **Daniel N. Moriasi:** Writing – review & editing, Supervision, Project administration, Funding acquisition.

Declaration of Competing Interest

The authors declare that they have no known competing financial interests or personal relationships that could have appeared to influence the work reported in this paper.

Data availability

The authors do not have permission to share data.

Acknowledgments

This research was supported in part by an appointment to the Agricultural Research Service (ARS) Research Participation Program

administered by the Oak Ridge Institute for Science and Education (ORISE) through an interagency agreement between the U.S. Department of Energy (DOE) and the U.S. Department of Agriculture (USDA). ORISE is managed by ORAU under DOE contract number DE-SC0014664. This research contributes to the Long-Term Agroecosystem Research (LTAR) Network and Conservation Effects Assessment Project (CEAP), two USDA national research networks. All opinions expressed in this paper are the author's and do not necessarily reflect the policies and views of USDA, DOE, or ORAU/ORISE. Mention of trade names or commercial products in this publication is solely for the purpose of providing specific information and does not imply recommendation or endorsement by the USDA. USDA is an equal opportunity provider and employer.

Appendix A. Supporting information

Supplementary data associated with this article can be found in the online version at doi:10.1016/j.ejrh.2024.101761.

References

AghaKouchak, A., Mirchi, A., Madani, K., Di Baldassarre, G., Nazemi, A., Alborzi, A., Anjileli, H., Azarderakhsh, M., Chiang, F., Hassanzadeh, E., Huning, L.S., Mallakpour, I., Martinez, A., Mazdiyasni, O., Moftakhari, H., Norouzi, H., Sadegh, M., Sadeqi, D., Van Loon, A.F., Wanders, N., 2021. Anthropogenic drought: definition, challenges, and opportunities. Rev. Geophys. https://doi.org/10.1029/2019RG000683.

Ahmadalipour, A., Moradkhani, H., Svoboda, M., 2017b. Centennial drought outlook over the CONUS using NASA-NEX downscaled climate ensemble. Int. J. Climatol. 37, 2477–2491. https://doi.org/10.1002/JOC.4859.

Ahmadalipour, A., Moradkhani, H., Demirel, M.C., 2017a. A comparative assessment of projected meteorological and hydrological droughts: Elucidating the role of temperature. J. Hydrol. (Amst. 553, 785–797. https://doi.org/10.1016/J.JHYDROL.2017.08.047.

Allen, R.G., Pereira, L.S., Raes, D., Smith, M., 1998. Crop evapotranspiration: Guidelines for computing crop requirements. Irrigation and Drainage Paper No. 56. FAO. https://doi.org/10.1016/j.eja.2010.12.001.

Amatya, D.M., Skaggs, R.W., Gregory, J.D., 1995. Comparison of Methods for Estimating REF-ET. J. Irrig. Drain. Eng. 121, 427–435. https://doi.org/10.1061/(ASCE)0733-9437(1995)121:6(427).

Basara, J.B., Maybourn, J.N., Peirano, C.M., Tate, J.E., Brown, P.J., Hoey, J.D., Smith, B.R., 2013. Drought and Associated Impacts in the Great Plains of the United States—A Review. Int. J. Geosci. 04, 72–81. https://doi.org/10.4236/ijg.2013.46a2009.

Beguería, S., Vicente-Serrano, S.M., Reig, F., Latorre, B., 2014. Standardized precipitation evapotranspiration index (SPEI) revisited: Parameter fitting, evapotranspiration models, tools, datasets and drought monitoring. Int. J. Climatol. 34, 3001–3023. https://doi.org/10.1002/joc.3887.

Berti, A., Tardivo, G., Chiaudani, A., Rech, F., Borin, M., 2014. Assessing reference evapotranspiration by the Hargreaves method in north-eastern Italy. Agric. Water Manag 140, 20–25. https://doi.org/10.1016/J.AGWAT.2014.03.015.

Brock, F.V., Crawford, K.C., Elliott, R.L., Cuperus, G.W., Stadler, S.J., Johnson, H.L., Eilts, M.D., 1995. The Oklahoma Mesonet: A Technical Overview. J. Atmos. Ocean Technol. 12. https://doi.org/10.1175/1520-0426(1995)012<0005:tomato>2.0.co;2.

Bussi, G., Whitehead, P.G., 2020. Impacts of droughts on low flows and water quality near power stations. Hydrol. Sci. J. 65 https://doi.org/10.1080/02626667.2020.1724295.

Chiang, F., Mazdiyasni, O., AghaKouchak, A., 2021. Evidence of anthropogenic impacts on global drought frequency, duration, and intensity, 2021 12:1 Nat. Commun. 12, 1–10. https://doi.org/10.1038/s41467-021-22314-w.

Christian, J., Christian, K., Basara, J.B., 2015. Drought and pluvial dipole events within the great plains of the United States. J. Appl. Meteor. Clim. 54, 1886–1898. https://doi.org/10.1175/JAMC-D-15-0002.1.

Cook, B.I., Mankin, J.S., Williams, A.P., Marvel, K.D., Smerdon, J.E., Liu, H., 2021. Uncertainties, Limits, and Benefits of Climate Change Mitigation for Soil Moisture Drought in Southwestern North America. Earths Future 9, e2021EF002014. https://doi.org/10.1029/2021EF002014.

Danandeh Mehr, A., Sorman, A.U., Kahya, E., Hesami Afshar, M., 2020. Climate change impacts on meteorological drought using SPI and SPEI: case study of Ankara, Turkey. Hydrol. Sci. J. 65, 254–268. https://doi.org/10.1080/02626667.2019.1691218.

Diffenbaugh, N.S., Swain, D.L., Touma, D., Lubchenco, J., 2015. Anthropogenic warming has increased drought risk in California. Proc. Natl. Acad. Sci. USA 112, 3931–3936. ⟨https://doi.org/10.1073/PNAS.1422385112/SUPPL_FILE/PNAS.201422385SI.PDF⟩.

Douris, J., Kim, G., Abrahams, J., Lapitan Moreno, J., Shumake-Guillemot, J., Green, H., Murray, V., 2021. WMO Atlas of Mortality and Economic Losses from Weather, Climate and Water Extremes (1970–2019) (WMO-No. 1267), WMO Statement on the state of the Global Climate.

Garbrecht, J.D., Starks, P.J., Steiner, J.L., 2006. The under-appreciated climate factor in the Conservation Effects Assessment Project. J. Soil Water Conserv 61, 110A–112A.

Gholizadeh, R., Yılmaz, H., Danandeh Mehr, A., 2022. Multitemporal meteorological drought forecasting using Bat-ELM. Acta Geophys. 70 https://doi.org/10.1007/s11600-022-00739-1.

Gill, J.C., Malamud, B.D., 2014. Reviewing and visualizing the interactions of natural hazards. Rev. Geophys. https://doi.org/10.1002/2013RG000445.

Gui, Y., Wang, Q., Zhao, Y., Dong, Y., Li, H., Jiang, S., He, X., Liu, K., 2021. Attribution analyses of reference evapotranspiration changes in China incorporating surface resistance change response to elevated CO2. J. Hydrol. (Amst.) 599, 126387. https://doi.org/10.1016/J.JHYDROL.2021.126387.

Guttman, N.B., 1998. Comparing the Palmer Drought Index and the Standardized Precipitation Index. JAWRA J. Am. Water Resour. Assoc. 34, 113–121. https://doi.org/10.1111/J.1752-1688.1998.TB05964.X.

Hargreaves, G.H., Samani, Z.A., 1985. Reference Crop Evapotranspiration from Temperature. Appl. Eng. Agric. 1, 96–99. https://doi.org/10.13031/2013.26773.

Jensen, M.E., Allen, R.G., 2016. Evaporation, Evapotranspiration, and Irrigation Water Requirements. Evaporation, evapotranspiration, Irrig. Water Requir. https://doi.org/10.1061/9780784414057.

Johnson, F., Sharma, A., 2015. What are the impacts of bias correction on future drought projections? J. Hydrol. (Amst. 525, 472–485. https://doi.org/10.1016/j.jhydrol.2015.04.002.

Lai, C., Zhong, R., Wang, Z., Wu, X., Chen, X., Wang, P., Lian, Y., 2019. Monitoring hydrological drought using long-term satellite-based precipitation data. Sci. Total Environ. 649 https://doi.org/10.1016/j.scitotenv.2018.08.245.

Lee, S., Ajami, H., 2023. Comprehensive assessment of baseflow responses to long-term meteorological droughts across the United States. J. Hydrol. (Amst.) 626 (Part A), 130256. https://doi.org/10.1016/j.jhydrol.2023.130256.

Li, M., Li, S., Liu, Q., Kang, Y., Liang, L., Yuan, X., Zhang, J., Wang, X., Li, C., 2022. Assessment of hydrological response to multiyear drought: Insights from lag characteristics and shift magnitude. Hydrol. Process 36. https://doi.org/10.1002/hyp.14636.

Liu, C., Yang, C., Yang, Q., Wang, J., 2021. Spatiotemporal drought analysis by the standardized precipitation index (SPI) and standardized precipitation evapotranspiration index (SPEI) in Sichuan Province, China. Sci. Rep. 11 https://doi.org/10.1038/s41598-020-80527-3.

Lloyd-Hughes, B., Saunders, M.A., 2002. A drought climatology for Europe. Int. J. Climatol. 22, 1571–1592. https://doi.org/10.1002/JOC.846.

Mann, H.B., Whitney, D.R., 1947. On a Test of Whether one of Two Random Variables is Stochastically Larger than the Other. Ann. Math. Stat. 18 https://doi.org/10.1214/aoms/1177730491.

McHugh, M.L., 2012. Interrater reliability: The kappa statistic. Biochem Med (Zagreb) 22. https://doi.org/10.11613/bm.2012.031.
McKee, T., Doesken, B., Kleist, J., 1993. The Relationship of Drought Frequency and Duration to Time Scales, in: The 8th Conference on Applied Climatology. Anaheim, California, pp. 179–183.
McPherson, R.A., Fiebrich, C.A., Crawford, K.C., Elliott, R.L., Kilby, J.R., Grimsley, D.L., Martinez, J.E., Basara, J.B., Illston, B.G., Morris, D.A., Kloesel, K.A., Stadler, S. J., Melvin, A.D., Sutherland, A.J., Shrivastava, H., Carlson, J.D., Wolfinbarger, J.M., Bostic, J.P., Demko, D.B., 2007. Statewide monitoring of the mesoscale environment: A technical update on the Oklahoma Mesonet. J. Atmos. Ocean Technol. 24 https://doi.org/10.1175/JTECH1976.1.
Meresa, H., Zhang, Y., Tian, J., Abrar Faiz, M., 2023. Understanding the role of catchment and climate characteristics in the propagation of meteorological to hydrological drought. J. Hydrol. (Amst.) 617, 128967. https://doi.org/10.1016/J.JHYDROL.2022.128967.
Monteith, J., 1965. Evaporation and environment. 19th Symposia of the Society for Experimental Biology. University Press, Cambridge, 205-234. Symp Soc Exp Biol.
Naresh Kumar, M., Murthy, C.S., Sesha sai, M.V.R., Roy, P.S., 2009. On the use of Standardized Precipitation Index (SPI) for drought intensity assessment. Meteorol. Appl. 16, 381–389. https://doi.org/10.1002/met.136.
Ortiz-Gómez, R., Flowers-Cano, R.S., Medina-García, G., 2022. Sensitivity of the RDI and SPEI Drought Indices to Different Models for Estimating Evapotranspiration Potential in Semiarid Regions. Water Resour. Manag. 36 https://doi.org/10.1007/s11269-022-03154-9.
Peterson, T.J., Saft, M., Peel, M.C., John, A., 2021. Watersheds may not recover from drought. Science 372 (1979), 745–749. https://doi.org/10.1126/SCIENCE.ABD5085/SUPPL_FILE/ABD5085S2.MP4.
Pyarali, K., Peng, J., Disse, M., Tuo, Y., 2022. Development and application of high resolution SPEI drought dataset for Central Asia. Sci. Data 9. https://doi.org/10.1038/s41597-022-01279-5.
Rajbanshi, J., Das, S., 2021. The variability and teleconnections of meteorological drought in the Indian summer monsoon season: Implications for staple crop production. J. Hydrol. (Amst. 603, 126845 https://doi.org/10.1016/J.JHYDROL.2021.126845.
Ramírez, A., Gutiérrez-Fonseca, P.E., Kelly, S.P., Engman, A.C., Wagner, K., Rosas, K.G., Rodríguez, N., 2018. Drought facilitates species invasions in an urban stream: Results from a long-term study of tropical island fish assemblage structure. Front Ecol. Evol. 6 https://doi.org/10.3389/fevo.2018.00115.
Saft, M., Peel, M.C., Western, A.W., Zhang, L., 2016. Predicting shifts in rainfall-runoff partitioning during multiyear drought: Roles of dry period and catchment characteristics. Water Resour. Res 52, 9290–9305. https://doi.org/10.1002/2016WR019525.
Schyns, J.F., Hoekstra, A.Y., Booij, M.J., 2015. Review and classification of indicators of green water availability and scarcity. Hydrol. Earth Syst. Sci. 19, 4581–4608. https://doi.org/10.5194/hess-19-4581-2015.
Sheffield, J., Wood, E.F., Roderick, M.L., 2012. Little change in global drought over the past 60 years, 2012 491:7424 Nature 491, 435–438. https://doi.org/10.1038/nature11575.
Stagge, J.H., Tallaksen, L.M., Xu, C.-Y., Van Lanen, H.A.J., 2014. Standardized precipitation-evapotranspiration index (SPEI): Sensitivity to potential evapotranspiration model and parameters. IAHS Publ.
Stagge, J.H., Tallaksen, L.M., Gudmundsson, L., Van Loon, A.F., Stahl, K., 2015. Candidate Distributions for Climatological Drought Indices (SPI and SPEI). Int. J. Climatol. 35, 4027–4040. https://doi.org/10.1002/joc.4267.
Strzepek, K., Yohe, G., Neumann, J., Boehlert, B., 2010. Characterizing changes in drought risk for the United States from climate change. Environ. Res. Lett. 5, 044012 https://doi.org/10.1088/1748-9326/5/4/044012.
Temesgen, B., Eching, S., Davidoff, B., Frame, K., 2005. Comparison of Some Reference Evapotranspiration Equations for California. J. Irrig. Drain. Eng. 131, 73–84. https://doi.org/10.1061/(ASCE)0733-9437(2005)131:1(73).
Teutschbein, C., Jonsson, E., Todorović, A., Tootoonchi, F., Stenfors, E., Grabs, T., 2023. Future drought propagation through the water-energy-food-ecosystem nexus – A Nordic perspective. J. Hydrol. (Amst.) 617, 128963. https://doi.org/10.1016/J.JHYDROL.2022.128963.
Thornthwaite, C.W., 1948. An Approach toward a Rational Classification of Climate. Geogr. Rev. 38, 55. https://doi.org/10.2307/210739.
Tian, L., Quiring, S.M., 2019. Spatial and temporal patterns of drought in Oklahoma (1901–2014). Int. J. Climatol. 39, 3365–3378. https://doi.org/10.1002/JOC.6026.
Tirivarombo, S., Osupile, D., Eliasson, P., 2018. Drought monitoring and analysis: Standardised Precipitation Evapotranspiration Index (SPEI) and Standardised Precipitation Index (SPI). Phys. Chem. Earth 106, 1–10. https://doi.org/10.1016/j.pce.2018.07.001.
Trajkovic, S., 2007. Hargreaves versus Penman-Monteith under Humid Conditions. J. Irrig. Drain. Eng. 133, 38–42. https://doi.org/10.1061/(ASCE)0733-9437(2007)133:1(38).
Trenberth, K.E., Dai, A., Van Der Schrier, G., Jones, P.D., Barichivich, J., Briffa, K.R., Sheffield, J., 2014. Global warming and changes in drought, 2014 4 Nat. Clim. Chang 4 (1), 17–22. https://doi.org/10.1038/nclimate2067.
Tripathy, K.P., Mukherjee, S., Mishra, A.K., Mann, M.E., Williams, A.P., 2023. Climate change will accelerate the high-end risk of compound drought and heatwave events. Proc. Natl. Acad. Sci. 120 (28), e2219825120 https://doi.org/10.1073/pnas.2219825120.
Van Der Schrier, G., Jones, P.D., Briffa, K.R., 2011. The sensitivity of the PDSI to the Thornthwaite and Penman-Monteith parameterizations for potential evapotranspiration. J. Geophys. Res. Atmospheres 116. https://doi.org/10.1029/2010JD015001.
Van Loon, A.F., 2015. Hydrological drought explained. Wiley Interdiscip. Rev.: Water 2, 359–392. https://doi.org/10.1002/WAT2.1085.
Vicente-Serrano, S.M., Beguería, S., 2016. Comment on "Candidate distributions for climatological drought indices (SPI and SPEI)" by James H. Stagge et al. Int. J. Climatol. 36, 2120–2131. https://doi.org/10.1002/joc.4474.
Vicente-Serrano, S.M., Beguería, S., López-Moreno, J.I., 2010. A Multiscalar Drought Index Sensitive to Global Warming: The Standardized Precipitation Evapotranspiration Index. J. Clim. 23, 1696–1718. https://doi.org/10.1175/2009JCLI2909.1.
Walter, I.A., Allen, R.G., Elliott, R., Jensen, M.E., Itenfisu, D., Mecham, B., Howell, T.A., Snyder, R., Brown, P., Echings, S., Spofford, T., Hattendorf, M., Cuenca, R.H., Wright, J.L., Martin, D., 2004. ASCE's Standardized Reference Evapotranspiration Equation. Watershed Manag. Oper. Manag. 105 (2000), 1–11. https://doi.org/10.1061/40499(2000)126.
Wang, Q., Zeng, J., Qi, J., Zhang, X., Zeng, Y., Shui, W., Xu, Z., Zhang, R., Wu, X., Cong, J., 2021. A multi-scale daily SPEI dataset for drought characterization at observation stations over mainland China from 1961 to 2018. Earth Syst. Sci. Data 13. https://doi.org/10.5194/essd-13-331-2021.
Wilhite, D.A., Glantz, M.H., 1985. Understanding: The drought phenomenon: The role of definitions. Water Int 10, 111–120. https://doi.org/10.1080/02508068508686328.
Williams, A.P., Seager, R., Abatzoglou, J.T., Cook, B.I., Smerdon, J.E., Cook, E.R., 2015. Contribution of anthropogenic warming to California drought during 2012–2014. Geophys Res Lett. 42, 6819–6828. https://doi.org/10.1002/2015GL064924.
WMO, 2006. Drought Monitoring and Early Warning: Concepts, Progress, and Future Challenges. WMO, WMO, Geneva.
Yao, J., Zhao, Y., Chen, Y., Yu, X., Zhang, R., 2018. Multi-scale assessments of droughts: A case study in Xinjiang, China. Sci. Total Environ. 630, 444–452. https://doi.org/10.1016/j.scitotenv.2018.02.200.
Zarei, A.R., Mahmoudi, M.R., 2020. Assessment of the effect of PET calculation method on the Standardized Precipitation Evapotranspiration Index (SPEI). Arab. J. Geosci. 13 https://doi.org/10.1007/s12517-020-5197-z.
Zhou, Z., Shi, H., Fu, Q., Ding, Y., Li, T., Wang, Y., Liu, S., 2021. Characteristics of Propagation From Meteorological Drought to Hydrological Drought in the Pearl River Basin. J. Geophys. Res.: Atmospheres 126, e2020JD033959. https://doi.org/10.1029/2020JD033959.